

Spontaneous vacancy array formation on FeSi₂ and CoSi₂ formed on Si(100) 2×*n* surface

Jun-Zhong Wang, Jin-Feng Jia, Hong Liu, Jian-Long Li, Xi Liu, and Qi-Kun Xue^{a)}

State Key Laboratory for Surface Physics, and International Center for Quantum Structures, Institute of Physics, the Chinese Academy of Sciences, Beijing 100080, People's Republic of China

(Received 12 December 2001; accepted for publication 28 January 2002)

Atomic structure of FeSi₂ or CoSi₂ grown on the Si(100) 2×*n* surface has been investigated by scanning tunneling microscopy. After annealing the Fe or Co covered Si(100) 2×*n* substrate at ~800 °C, an ordered adatom vacancy array appears on the nominal 1×1 surface of the formed FeSi₂ or CoSi₂ islands, which has not been observed for silicide on the Si(100)-2×1. Upon further annealing to ~1100 °C, the vacancies coalesce into striped domains along one of the ⟨011⟩ directions. These nanostructured features are a result of the Ni impurities, and can be a promising template for fabricating nanodot arrays. © 2002 American Institute of Physics.

[DOI: 10.1063/1.1461904]

Ferromagnetic metal silicides grown epitaxially on Si have attracted great interest in the past decade due to their importance in microelectronics. Among them CoSi₂ and NiSi₂ are by far the most studied systems.¹ CoSi₂ is attractive as a self-aligned silicide for high-performance ultralarge scale integrated devices because of its low lattice mismatch with Si (-1.2%) and low electrical resistivity (14 μΩ cm) at room temperature (RT).^{2,3} Compared with other silicides, FeSi₂ is more interesting because it exists in four different phases with distinct properties denoted as α, β, pseudomorphic, and γ-FeSi₂, respectively. γ-FeSi₂ has a CaF₂ structure of metallic character with a lattice constant ~*a*_{Si}=5.43 Å.^{4,5}

In the growth of various epitaxial layers, defects play very important roles in determining qualities of the grown layers. The dimer vacancy lines (DVLs) giving rise to the 2×*n* structure on Si(100) are one of the well known defects in this category.⁶⁻¹⁰ A tiny amount of metal contaminations, like Ni, can lead to dimer vacancies to coalesce into DVLs.^{11,12} The ordering of dimer vacancies is driven by a short-range attractive interaction between vacancies in adjacent dimer rows, and by a long-range repulsive interaction between vacancies in the same row.¹³ Zandvliet *et al.*¹⁴ have shown that the long-range repulsive interaction is related to strain relaxation.

Owing to a big difference in defect density between the Si(100) 2×*n* and 2×1 surfaces, it is expected that growth and structure of silicides on two surfaces should differ significantly. Recently, Goldfarb and Briggs¹⁵ have found two different reconstructions for the CoSi₂ islands on the 2×*n* and vicinal 2×1 substrates: 3D islands with a *c*(2×4) structure on the former, while 2D platelets with a *p*(2×2) + *c*(2×2) mixed phases on the latter.

In this letter, we report ordered adatom vacancy array on the FeSi₂ or CoSi₂ islands that are grown on the Si(100) 2×*n* substrate by molecular beam epitaxy (MBE). Such an array does not appear on the silicides formed on the Si(100) 2×1 substrate. Although similar vacancy array on NiSi₂ was

reported previously,¹⁶⁻¹⁸ it is difficult to determine whether such an array is an intrinsic feature of the Ni silicide. This work shows that vacancy array is a common phenomenon for the ferromagnetic metal silicides grown on Si(100) 2×*n*, and its formation can be controlled easily by a small amount of certain dopants such as Ni.

The experiments were performed on a commercial Omicron ultrahigh vacuum (UHV) variable temperature scanning tunneling microscope (STM), equipped with a low energy electron diffraction (LEED)/Auger spectrometer with a base pressure of 5.0×10⁻¹¹ mbar. The STM images were obtained in the constant-current mode with electrochemically etched W tips. The sample used was a heavily P-doped Si (001) wafer with a resistivity of ~0.001 Ω cm, which was intentionally contacted to a stainless steel tweezer before loaded into the UHV system. The small amount of Ni contamination from the contact was found to be enough to produce the Si(100) 2×*n* structure as described in Ref. 19. To prepare a clean surface, the sample was flashed up to 1150 °C in the UHV chamber for several seconds, maintaining the pressure better than 10⁻⁹ mbar. A well ordered 2×*n* structure can be achieved with 15-20 cycles of flashing.

A water-cooled *e*-beam bombardment evaporator was used to deposit Fe, while Co was deposited by direct current heating of a W wire coated with Co film by electrodeposition. Fe or Co silicides were prepared by subsequent annealing to specified temperatures, which were measured by an infrared pyrometer.

Figure 1(a) shows the STM image of the as-prepared 2×*n* surface, which is characterized by the DVLs perpendicular to the dimer rows. The DVLs pervade the whole surface with fairly good spatial periodicity. For most samples we studied, *n* varies from 8 to 12.²⁰

~2 Å Fe was then deposited on the above 2×*n* surface at RT. After subsequent annealing at 800 °C for 5 min, Fe silicide islands with an orientation parallel to the ⟨011⟩ directions were observed. The typical morphology includes both 3D islands with flat tops and faceted huts, similar to the observation by Goldfarb and Briggs.¹⁵ According to Behar *et al.*,⁴ the Fe silicide formed at 800 °C can be identified as

^{a)}Electronic mail: qkxue@aphy.iphy.ac.cn

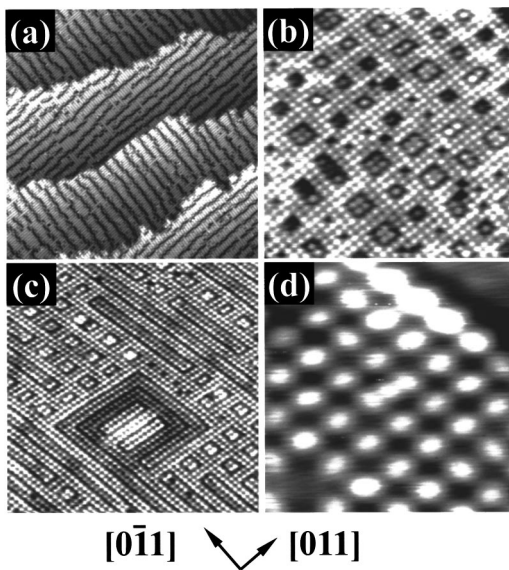


FIG. 1. (a) Typical STM image of as-prepared Si(100) $2 \times n$ surface ($100 \times 100 \text{ nm}^2$, $V_s = -2.0 \text{ V}$, $I = 0.03 \text{ nA}$); (b) atomic resolution image of the FeSi_2 islands after annealing at $800 \text{ }^\circ\text{C}$ ($14 \times 14 \text{ nm}^2$, $V_s = -0.67 \text{ V}$, $I = 1.0 \text{ nA}$); (c) FeSi_2 island after annealing at $1100 \text{ }^\circ\text{C}$ ($20 \times 20 \text{ nm}^2$, $V_s = -0.55 \text{ V}$, $I = 0.5 \text{ nA}$); (d) FeSi_2 island formed on Si(100) 2×1 after annealing at $800 \text{ }^\circ\text{C}$ for 5 min ($8 \times 8 \text{ nm}^2$, $V_s = 3.2 \text{ V}$, $I = 0.028 \text{ nA}$).

the FeSi_2 phase. The atomic resolution image of the 3D islands is shown in Fig. 1(b), where the adatom vacancy array appears on the islands with vacancy sizes of $a_0 \times a_0$, $2a_0 \times 2a_0$, $2a_0 \times 3a_0$, $3a_0 \times 3a_0$, etc. Within the vacancies, there are some abnormal adatoms, which are shifted by 1.9 \AA (the half unit cell) along the $[011]$ and $[0\bar{1}1]$ directions with respect to the surrounding normal adatoms. Hereafter we refer to the former as “center atoms,” and the latter as “frame atoms.”¹⁸ The vacancies usually contain four center atoms, and vacancies with 0, 1, or 2 protrusions are also observed. Interestingly, there are no more than two adjacent adatoms to align simultaneously along the $[011]$ and $[0\bar{1}1]$ directions. Unlike the case on $2 \times n$ surface, the vacancies are not connected together to form lines. This suggests that, at the annealing temperature, although some adatom vacancies are mobile, the short-range attractive interaction between the adjacent vacancies is not strong enough to overcome the thermal fluctuation. In addition, both the center and frame atoms have a nearest-neighboring distance of 3.8 \AA , the same as the lattice constant of $\gamma\text{-FeSi}_2$ (100) so this Fe disilicide can be recognized as the $\gamma\text{-FeSi}_2$ phase.

After further annealing the sample up to $\sim 1100 \text{ }^\circ\text{C}$, the island number significantly decreases at an expense of increasing island sizes. The atomic resolution image is shown in Fig. 1(c), where the vacancy array becomes much ordered. More interestingly, some vacancy patches connect each other along one of the $\langle 011 \rangle$ directions, forming a straight stripe with a width of $3a_0$. In term of the above two annealing temperatures, we can infer that the barrier height for the coalesce of adatom vacancy ranges from ~ 70 to $\sim 90 \text{ meV}$. This striped domain is very similar to the DVLS on the Si(100) $2 \times n$ surface. The difference lies in a monotonic width of $3a_0$ and the embedded center atoms for the former. As the striped vacancy domains are straight, we speculate the long-range repulsive interaction between vacancies to be

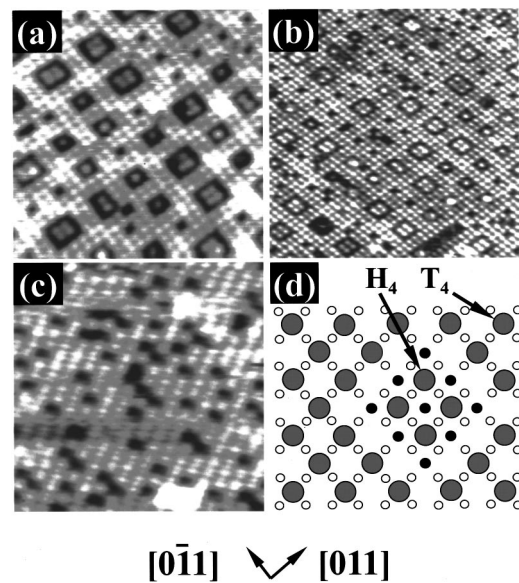


FIG. 2. (a),(b) Atomically resolved STM images of the CoSi_2 island on Si(100) $2 \times n$ surface after annealing at $800 \text{ }^\circ\text{C}$, (a) $12 \times 12 \text{ nm}^2$ ($V_s = -1.14 \text{ V}$, $I = 0.036 \text{ nA}$); and (b) $17 \times 17 \text{ nm}^2$ ($V_s = -0.44 \text{ V}$, $I = 0.04 \text{ nA}$); (c) CoSi_2 island grown on Si(100) 2×1 ($10.5 \times 10.5 \text{ nm}^2$, $V_s = -1.0 \text{ V}$, $I = 0.04 \text{ nA}$); (d) top view of the structure model proposed for the vacancy array. The hatched and solid circles denote Si adatoms and Fe (Co) atoms, respectively. The open circles correspond to the second layer Si.

stronger than that on the Si(100) $2 \times n$. This feature can be understood based on the fact that the long-range interaction decays as L^{-2} .¹⁴ For the striped vacancies, L equals to $3a_0$, much less than na_0 of the Si(100) $2 \times n$ ($n \geq 8$ in our case). As a consequence, the striped vacancies become more ordered than the $2 \times n$.

We also deposited the same amount of Fe on the Si(100) 2×1 surface with similar annealing procedure. In this case, no vacancy array, but only a 3×3 reconstruction is observed, as shown in Fig. 1(d). Since the difference between the $2 \times n$ and 2×1 is in the DVLS, the formation of the vacancy array must be a result of the defects induced by the Ni contamination.

To understand the formation of the vacancy array, we carried out a similar experiment with Co. The Co silicide islands with heights of $3.5\text{--}4.0 \text{ nm}$ are formed, and most of them have a flat top. As CoSi_2 phase appears around $500 \text{ }^\circ\text{C}$, the observed silicides can be identified as the CoSi_2 phase.²¹ The high resolution images under different biases are shown in Figs. 2(a) and 2(b), in which the vacancy features are very similar to that of $\gamma\text{-FeSi}_2$. Both the frame and center atoms have a nearest-neighboring distance of 3.8 \AA , the lattice constant of the CoSi_2 (100) surface. Some vacancies with three protrusions can be observed occasionally. For comparison, the same amount of Co were deposited on the Si(100) 2×1 surface. After annealing at $800 \text{ }^\circ\text{C}$ for 5 min, CoSi_2 forms and the high resolution STM image is shown in Fig. 2(c). Instead of the ordered vacancy array, only small point defects without center atoms appear randomly on the CoSi_2 surface. These results are similar to the observation by Siringhaus, Lee, and Känel,^{22,23} where the $\sqrt{2} \times \sqrt{2} R45^\circ$ reconstruction of S surface was also observed. The experiment suggests that the formation of vacancy array on CoSi_2 is also related to the dimer defects on the $2 \times n$ substrate.

Three structure models were previously proposed to account for the vacancy arrays on NiSi₂ islands.^{16–18} In the model by Ono *et al.*,¹⁸ the NiSi₂ surface was supposed to be similar to the C surface of CoSi₂, i.e., the Si adatoms are located at the bridge sites of the second layer Ni. Khang and Kuk¹⁷ suggested the stacking fault to be the main mechanism for the vacancy array formation, and assigned the first layer to be Co atoms. However, the AES measurement indicated that the surface of NiSi₂ is Si-rich compared to bulk NiSi₂.¹⁶

As γ -FeSi₂, CoSi₂, and NiSi₂ all have the same CaF₂ structure with a lattice constant of 3.8 Å on the (100) plane, the structure model of the vacancy array should be very similar. We cannot rule out the possibility of the stacking fault model by Khang and Kuk, but we find that the model by Becker *et al.*¹⁶ can best explain our observations. As illustrated in Fig. 2(d), there are 1.5 ML of Si on top of the upper Fe or Co layer, with the frame atoms located at the T₄ site and the center atoms at H₄ site.

In summary, we have studied the surface structures of Fe and Co silicides grown on the Si(100) 2×*n* and 2×1 surfaces, respectively. Ordered vacancy array forms on both FeSi₂ and CoSi₂ surfaces when the Si(100)–2×*n* substrate is used. In contrast, vacancy array is absent for the silicides grown on the Si(100) 2×1. Such an array is found to be a common feature for ferromagnetic metal silicides formed on Si(100) 2×*n*, and is closely related to the DVLs induced by Ni contamination. Upon annealing further to 1100 °C, some vacancies coalesce into stripes along one ⟨011⟩ direction. There are no more than two adjacent adatoms to align simultaneously along both the principal directions. We emphasize that upon further optimization, this array can be a useful template for growing nanodot arrays.

This work is supported by the Natural Science Foundation of China under Grant Nos. 69625608 and 60076009.

- ¹S. Mantl, *Mater. Sci. Rep.* **8**, 1 (1992).
- ²S. P. Murarka, *Silicides for VLSI Applications* (Academic, New York, 1983).
- ³R. T. Tung and K. Inoue, in *Microscopy of Semiconducting Materials* (Institute of Physics, London, 1997), Vol. 157, p. 487.
- ⁴M. Behar, H. Bernas, J. Desimmoni, X. W. Lin, and R. L. Maltez, *J. Appl. Phys.* **79**, 752 (1996).
- ⁵A. L. Vazquez de Parga, J. de la Figuera, C. Ocal, and R. Miranda, *Europhys. Lett.* **18**, 595 (1992).
- ⁶J. A. Martin, D. E. Savage, W. Moritz, and M. G. Lagally, *Phys. Rev. Lett.* **56**, 1936 (1986).
- ⁷X. Chen, F. Wu, Z. Zhang, and M. G. Lagally, *Phys. Rev. Lett.* **73**, 850 (1994).
- ⁸F.-K. Men, A. R. Smith, K.-J. Chao, Z. Zhang, and C.-K. Shih, *Phys. Rev. B* **52**, R8650 (1995).
- ⁹M. H. Tsai, Y. S. Tsai, C. S. Chang, Y. Wei, and I. S. T. Tsong, *Phys. Rev. B* **56**, 7435 (1997).
- ¹⁰K. Muller, E. Lang, L. Hammer, W. Grimm, P. Heilmann, and K. Heinz, in *Determination of Surface Structure by LEED*, edited by P. M. Marcus and F. Jona (Plenum, New York, 1984), p. 483.
- ¹¹H. Niehus, U. K. Köhler, M. Copel, and J. E. Demuth, *J. Microsc.* **152**, 735 (1988).
- ¹²K. Kato, T. Ide, S. Miura, A. Tamura, and T. Ichinokawa, *Surf. Sci.* **194**, L87 (1988).
- ¹³P. C. Weakliem, Z. Zhang, and H. Metiu, *Surf. Sci.* **336**, 303 (1995).
- ¹⁴H. J. W. Zandvliet, H. K. Louwmsma, P. E. Hegeman, and B. Poelsema, *Phys. Rev. Lett.* **75**, 3890 (1995).
- ¹⁵I. Goldfarb and G. A. D. Briggs, *Phys. Rev. B* **60**, 4800 (1999).
- ¹⁶R. S. Becker, A. J. Becker, J. Sullivan, and R. T. Tung, *J. Vac. Sci. Technol. B* **11**, 752 (1993).
- ¹⁷Y. Khang and Y. Kuk, *Phys. Rev. B* **53**, 10775 (1996).
- ¹⁸I. Ono, M. Yoshimura, and K. Ueda, *J. Vac. Sci. Technol. B* **16**, 2947 (1998).
- ¹⁹J.-Y. Koo, J.-Y. Yi, C. Huang, D. Kim, and S. Lee, *Phys. Rev. B* **54**, 10308 (1996).
- ²⁰J.-L. Li, X.-J. Liang, J.-F. Jia, X. Liu, J.-Z. Wang, E.-G. Wang, and Q.-K. Xue, *Appl. Phys. Lett.* **79**, 2826 (2001).
- ²¹B. Voigtänder, V. Scheuch, H. P. Bonzel, S. Heinze, and S. Blügel, *Phys. Rev. B* **55**, R13444 (1997).
- ²²H. Siringhaus, E. Y. Lee, and H. von Känel, *Phys. Rev. Lett.* **74**, 3999 (1995).
- ²³R. Stalder, C. Schwarz, H. Siringhaus, and H. von Känel, *Surf. Sci.* **271**, 355 (1992).